

NUMERICAL COMPUTATIONS OF WAKE  
VORTICES BEHIND LIFTING SURFACES

A. Mattei and E. Santoro  
Aeritalia, Aerod. Group Naples, Italy

Abstract

A numerical method is developed for the calculation of the wake vortices behind lifting wings. According to modern three-dimensional methods, discrete vortices are distributed on the camber surface of the wing and upon the wake.

The rolled-up vortex sheet is obtained by a convergent iterative procedure. Different numerical schemes investigated are compared for obtaining smooth solutions and minimizing computer time.

I. Introduction

A method is described to evaluate the vortex sheet location behind lifting wing in subsonic potential steady flow. Several numerical problems have been checked to find a general method of solution and, at same time, non expensive for the computer running cost.

The method is from an arrangement of the VLM (Vortex Lattice Method) with the known assumption that the free vortices coincide with streamlines leaving the Trailing Edge (T.E.).

The non linearity of the wake problem depends on the unknowledge "a priori" of the wake correct location itself. Since the boundary external to wing - where the kinematic condition must be applied - is unknown, an indirect iterative numerical method of resolution needs. The kinematic condition, as well known, requires flow to be tangential to the vortex wake boundary: this imposition prevents flow through the wake boundary which is a streamline.

The basic numerical problem associated to non linearity is to get a rapid convergent simulation of the boundary surfaces at each cycle of computation and this follows from spanwise panel distribution, kind of streamline equation, integration technique and so on.

In this paper all the above mentioned open problems have been critically investigated within systematic numerical experiments. The final result is a general method easy to use, not expensive for the computer running cost and directly expanding to different three-dimensional flow conditions.

II. Description of the method

Since the basic equations and the singularity techniques for the numerical solutions of two- and three-dimensional potential flow are well known, let us consider, for brevity reason, the principal points of a potential wake computation:

- A convenient initial vortex wake is assigned.
- I) The strengths of the bounded vortices are calculated, see fig. 1.
- II) The streamlines leaving the T.E. in the same points from which the free vortices start, are determined.
- III) The wake vortices are disposed on the streamlines obtained by the step I, see fig. 2.

Iterating steps I, II, III until the free vortices sheet position doesn't change any more, the solution may be reached.

A part from some small variations due to Kutta condition imposed according to Mangler and Smith [9], the wake location doesn't seem to depend on the accuracy of the wing surface singularities simulation. So an "exact" three-dimensional wing panel method doesn't need; however following the preliminary discussions and the results obtained for cambered wing sections [19 & 21], in the step I bounded vortices and fixed control points are not situated on the planform but on the camber surface

wing. Till now the method has been applied to thickless wing.

When the strength of the bounded vortices are obtained - in each cycle - it's possible to evaluate the induced velocity components in the wake control points  $P_{ij}$ , see fig. 2:

$$\begin{aligned} u &= u(x_{ij}, y_{ij}, z_{ij}) \\ v &= v(x_{ij}, y_{ij}, z_{ij}) \\ w &= w(x_{ij}, y_{ij}, z_{ij}) \end{aligned} \quad (1)$$

and the derivatives:

$$\begin{aligned} \frac{dz}{dx} &= z'(x_{ij}, y_{ij}, z_{ij}) = \frac{W}{U} \\ \frac{dy}{dx} &= y'(x_{ij}, y_{ij}, z_{ij}) = \frac{V}{U} \end{aligned} \quad (2)$$

where:

$$\begin{aligned} U &= V_{\infty x} + u \approx V_{\infty x} \\ V &= V_{\infty y} + v \\ W &= V_{\infty z} + w \end{aligned}$$

are the components of the free stream velocity  $V_{\infty}$  in the points  $P_{ij}$ . The equations system (2) - which represent the streamlines - has the following initial condition at the T.E.:

$$\begin{aligned} X_{1,j} &= X_{TE,j} \\ Y_{1,j} &= Y_{TE,j} \\ Z_{1,j} &= Z_{TE,j} \quad (j = 1, NS+1) \end{aligned} \quad (3)$$

where NS is the number of strips in which the wing has been divided.

Integration equations (2), the streamlines leaving the T.E. are determined. These will form the wake boundary for the next cycle.

Several integration techniques for the equations (2) have been investigated: the two most significant are described below.

#### A. Full Lattice Integration

In the firsts techniques named "full lattice" (FLT), the induced velocities are calculated in all points  $P_{ij}^k$  of the wake lattice - at the cycle  $k$  - and the streamlines are integrate by the formulae:

$$\begin{aligned} z_{ij}^k &= z_{i-1,j}^{k-1} + \frac{W}{U} (x_{i-1,j}^{k-1}; \\ & \quad y_{i-1,j}^{k-1}; z_{i-1,j}^{k-1}) \Delta x_{i-1} \\ y_{ij}^k &= y_{i-1,j}^{k-1} + \frac{V}{U} (x_{i-1,j}^{k-1}; \\ & \quad y_{i-1,j}^{k-1}; z_{i-1,j}^{k-1}) \Delta x_{i-1} \end{aligned} \quad (4)$$

$$(i = 1, MW+1; j = 1, NS+1)$$

where:

$$\Delta x_{i-1} = x_{i,j}^0 - x_{i-1,j}^0$$

Here and in the following the superscript (0) refers to the position of the initial wake configuration. The abscissae of the points  $P_{ij}^k$  are supposed to be always the same during the iteration process.

Fig. 3 shows the wake rolling-up "story" at the station  $x/c_r = 6$  for a rectangular wing with  $R = 6$  and angle of attack  $\alpha = 10^\circ$ . Another example of the iteration scheme is shown in fig. 4.

#### B. Row by Row Integration

The second technique, the "row by row" (RRT) is the following.

At the first cycle, considering - for example - a planar wake parallel to  $V_{\infty}$ , the velocity in every points  $P_{1,j}^0$  ( $j = 1, NS + 1$ ) at the T.E. is calculated. Note that the T.E. points are fixed at every cycles. Hence, from the equations (2), the displacement of the points  $P_{2,j}^0$  and then their new position  $P_{2,j}^1$  ( $j = 1, NS+1$ ) is obtained.

Keeping unaltered the strengths of the singularities, the free vortices are disposed from  $P_{1,j}^0$  to  $P_{2,j}^1$ , and from  $P_{2,j}^1$  to infinity in the same direction of  $V_{\infty}$ , see sketch (a) of fig. 5. By this configuration the velocities in the points  $P_{2,j}^1$  are computed and then the positions of  $P_{3,j}^1$  are determined ... and so on till the points  $P_{MW+1,j}^1$  of the last considered row.

Sketch (b) of fig. 5 shows the situation at cycle  $k > 1$  when the velocity at the point  $P_{i,j}^k$  are calculated. In this case the polygonal vortex line ( $P_{1,j}^0; P_{2,j}^1; \dots; P_{i,j}^k; P_{i+1,j}^{k-1}; P_{i+2,j}^{k-1}; \dots$ ) is considered.

### III. Numerical results and fundamental aspects of the method

In the figg. 6 + 9 some results obtained for planar and flapped wings are presented. Fig. 10 shows a comparison between the final result obtained by the two integration techniques; the difference is essentially due to the different number of panels employed. But it is necessary to observe that the cycles number is higher for the FLT: nearly twice for the same number of wake panels NW.

Fig. 11 shows the CPU time/cycle versus NW for the UNIVAC 1106 system.

Fig. 12 shows the very high convergence speed of the RRT which other is very sensitive to the spanwise panel distribution as we'll see below.

In the fig. 13 is represented the rolling-up "story" obtained by the FLT for a non planar wing with  $R = 3$  at  $\alpha = 10^\circ$ . It shows slow convergence speed but, at same time, good convergence in spite of the confused evolution of the rolling-up in the first three cycles.

For the FLT, starting from a non planar assigned wake, numerical tests have shown that higher convergence speed, but sometimes less smoothness in the solution, can be obtained. The reason may be explained as follows.

The sketch (a) of the fig. 14 shows the position reached by the points  $P_{z,j}^o$  ( $j=1, NS+1$ ) - at the first cycle - when we start from a planar wake. In fact, the induced velocities are all parallel to the z axis and determine stronger displacements along z axis as station x increases ( $i \gg$ ) especially at the wing tip.

Now in the RRT, yet at the first cycle, the locations of the points  $P_{z,j}^1$  (and hence the associated induced velocities) follow more rapidly the true wake configurations. Their displacements induce velocity components along y axis which accelerate the rolling-up process, see sketch (b) of fig. 14. However with RRT the y-components may cause jumps and/or cross-over of the rolling sheets (see for example fig. 15) if an appropriate spanwise division isn't used, as shown later.

A proof of the higher convergence speed explanation is from the FLT results for a flapped wing which reaches more rapidly (three cycles) the final convergent wake solution than a planar one (seven cycles) with the same  $R$  and  $\alpha$ , of figg. 7 & 8.

### IV. Numerical problems

#### A. Spanwise panel distribution criterium

For the RRT the spanwise division criterium is determinant to obtain a smooth solution for rolled-up vortex sheet, without jumping or escaping points and cross-over.

Generally the spanwise cuts must be thick at the tip of the wing. In this region indeed we find strongest variations of vorticity  $\gamma = d\Gamma/dy$  which determines the rolling-up process. Since the free vortex strength is  $d\Gamma$  it is plausible to choose the spanwise panel distribution in the manner that  $d\Gamma = d\Gamma/dy dy = \gamma dy = \text{const.}$  Otherwise non regular solutions for the wake may happen. In fact this assumption assures, at least, that the velocities induced on two contiguous free vortices, at a given downstream station x, are of the same numerical magnitude. With  $d\Gamma = \text{const.}$  standard spanwise division formulae may be obtained in the following manner.

For a given circulation distribution  $\Gamma(y)$  on a wing semispan (=1.) the total  $\Gamma_t$  is given by:

$$\Gamma_t = \int_0^1 \gamma(y) dy \quad (5)$$

where  $\gamma(y) = d\Gamma(y)/dy$  is the free vorticity.

Subdivide now the wing semispan in NS strips so that for two contiguous stations  $y_i$  and  $y_{i+1}$  will be:

$$\int_{y_i}^{y_{i+1}} \gamma(y) dy = \text{const.} \quad (6)$$

From (5) and (6)

$$\Gamma_t = \sum_{i=1}^{NS} \int_{y_i}^{y_{i+1}} \gamma(y) dy \quad (7)$$

For solving this equation we may suppose that the derivative of the function has an exponential pattern:

$$\gamma = K \gamma^\beta \quad (8)$$

By (8) and (5):

$$K = (\beta + 1) \Gamma_t \quad (9)$$

and from (6):

$$\int_{\gamma_i}^{\gamma_{i+1}} \gamma(\gamma) d\gamma = \frac{\Gamma_t}{NS} \quad (10)$$

By putting (8) and (9) in (10) we have:

$$\gamma_{i+1} = \left[ \frac{1}{NS} + \gamma_i^{(\beta+1)} \right]^{\frac{1}{\beta+1}} \quad (11)$$

or:

$$\gamma_{i+1} = \left( \frac{i}{NS} \right)^{\frac{1}{\beta+1}} \quad (12)$$

with  $\gamma_1 = 0$  and  $\gamma_{NS+1} = 1$ .

Posing for simplicity:  $\beta = 0, 1, 2$  respectively, we obtain three different division laws A, B, C sketched in fig. 15.

Fig. 16 (a - b - c) shows several rolls-up obtained by RRT with A, B, C division laws. Numerical experiments have shown C law division most convenient from the computer time point of view.

However when the strips number NS increases beyond a certain limit NS\* (depending essentially on  $R$  and  $\alpha$ ) no smooth curve solutions appear, see fig. 16 (d).

#### B. Streamwise and chordwise panel distribution. $C_L$ computation

The streamwise panel distribution on the wake is much less critical than spanwise division as it results from the numerical experiments. Four streamwise panels are sufficient for  $1 \leq x/c \leq 1.5$ .

For the rolled-up vortex sheet evaluation the number of panels per strip on the wing has not great influence, especially for an uncambered wing since the wake location depends essentially on the spanwise more than on the chordwise load. The chordwise panel number influence on the  $\Gamma(y)$  distribution

is well known from VLM.

That the free vortices exact position doesn't affect the wing values may be seen from Table 1.

CYCLE	$C_L$
0	.76306
1	.76327
2	.76205
3	.76310
4	.76278

TABLE 1  $C_L$  VARIATIONS

#### V. CONCLUSIONS

The described method appear easy to use and it can be placed among the three-dimensional methods for the aerodynamic analysis of the airplanes (from the VLM to the Three-dimensional Panel Method). It can be extended to other three-dimensional potential flows.

Two different numerical schemes (FLT & RRT) for determining wake locations have been examined and compared. The principal results of this study are:

- With the FLT technique regular rolling-up vortex sheets are obtained, but the convergence speed is low if an oportune initial wake configuration isn't used.
- Indeed with RRT approach no smooth and/or convergent solutions are available if "non suitable" spanwise panel distribution is used. Conversely if it is convergent, the computing time is about 1/2 of the FLT technique starting from a planar wake.

#### VII. ACKNOWLEDGMENTS

The authors wish to thank "Aeritalia" for the permission to publish this paper.

They express their gratitude to Dr. M. Travaglione of the Computer Center of Aeritalia Naples for his consistent help to prepare the pertinent programs.

The authors are grateful to Prof. Luigi G. Napolitano and Prof. V. Losito (Institute of Aerodynamics - University of Naples) for their constructive suggestions and comments.

### VIII. List of symbols

$R$	aspect ratio
$c$	chord length
$c_R$	root chord length
$K$	constant in the free vorticity assigned law
$MW$	number of horizontal streamwise wake strips
$NC$	number of chordwise panels on the wing
$NS$	number of vertical spanwise wing strips
$P$	point of the wake lattice
$x, y, z$	reference coordinate system
$u, v, w$	velocity components induced by bounded and free vortices
$U, V, W$	total velocity components
$\underline{V}_\infty$	free stream velocity vector
$\alpha$	angle of attack
$\beta$	free vorticity law exponent
$\gamma$	free vorticity
$\Gamma$	circulation around wing section
$\delta$	vortex core diameter
$\Delta x$	streamwise stepsize
$\Delta y$	spanwise stepsize
$\lambda$	taper ratio
$\Lambda$	swept angle

#### Subscripts

$i, j$	refers to $j$ -th point of the wake lattice counted from the trailing edge on $i$ -th vortex of the wing span
LE	refers to leading edge
TE	refers to trailing edge

#### Superscripts

$k$	refers to the $k$ -th cycle of the iteration
'	refers to the derivative respect to $x$
$o$	refers to the initial wake configuration

### BIBLIOGRAPHY

- 1 C.E. Brown: Aerodynamics of Wake Vortices, AIAA J., Vol. 11, No. 4, April 1973
- 2 A.H. Logan: Vortex Velocity Distributions at Large Downstream Distances, J. Aircraft, Vol. 8, No. 11
- 3 V.J. Rossow: On the Inviscid Rolled-Up Structure of Lift-Generated Vortices, J. Aircraft, Vol. 10, No. 11 .
- 4 I. Tombach: Observations of Atmospheric Effects on Vortex Wake Behavior, J. Aircraft, Vol. 10, No. 11
- 5 J.E. Hackett, M.R. Evans: Vortex Wakes Behind High-Lift Wings, J. Aircraft, Vol. 8, No. 5
- 6 P.F. Jordan: Structure of Betz Vortex Cores, J. Aircraft Vol. 10, No. 11
- 7 W.H. Mason, J.F. Marchman: Far Field Structure of Aircraft Wake Turbulence, J. Aircraft, Vol. 10, No. 2
- 8 H. Chevalier: Flight Test Studies of the Formation and Dissipation of Trailing Vortices, J. Aircraft, Vol. 10, No. 1
- 9 K.W. Mangler, J.H.B. Smith: Behaviour of the Vortex Sheet at the Trailing Edge of a Lifting Wing, R.A.E. T.N. 69049
- 10 G.J. Hancock; On the Rolling-Up of a Trailing Vortex Sheet, Aeronautical J. of R.A.S., Vol. 74
- 11 Th.A. Mc Mahon: Review of the Vortex Wake Roll-Up Problem, ASRL TR 145-1
- 12 F.L. Westwater: Rolling-Up of the Surface of Discontinuity behind an aerofoil of Finite Span, A.R.C., R & M 1692
- 13 D.J. Butter, G.J. Hancock: A Numerical Method for calculating the Trailing Vortex System behind a Swept Wing at Low Speed, Aeronautical J. of R.A.S., Vol. 75, August 1971
- 14 C.D. Cone: A Theoretical Investigation of Vortex Sheet Deformation Behind a Highly Loaded Wing and its Effect on Lift, NACA TN D-657
- 15 T.E. Labruiere: A Numerical Method for the Determination of the Vortex Sheet Location behind a Wing in Incompressible Flow, NLR TR 72091 U
- 16 J. Rom, C. Zorea: The Calculation of the Lift Distribution and the Near Vortex Wake Behind High and Low Aspect Ratio Wings in Subsonic Flow, T.A.E. Rep. No. 168

- 17 R. Legendre: Effect of Wing Tip Shape On Vortex Sheet Rolling-Up, ONERA, August 1971
- 18 C. Rehback: Numerical Study of the Influence of the Wing Tip Shape on the Vortex Sheet Rolling-Up, ONERA, Nov. 1971
- 19 A. Mattei: Distribuzione discreta di vortici lungo la linea media di profili sottili, Convegno AIDAA Torino, June 1972 (Unpublished)
- 20 A. Mattei: Metodo non lineare per il design di linee medie di profili alari. Congresso AIDAA Pisa, Sept. 1973 (Unpublished)
- 21 V. Losito: Analisi e disegno di profili sottili e molto ricurvi. Congresso AIDAA Pisa, Sept. 1973 (Unpublished)
- 22 V. Losito, A. Mattei, L.G. NAPOLITANO: On Two and three-dimensional Singularity. Paper to be published on AIDAA J., Sept. 1974

# STEP I

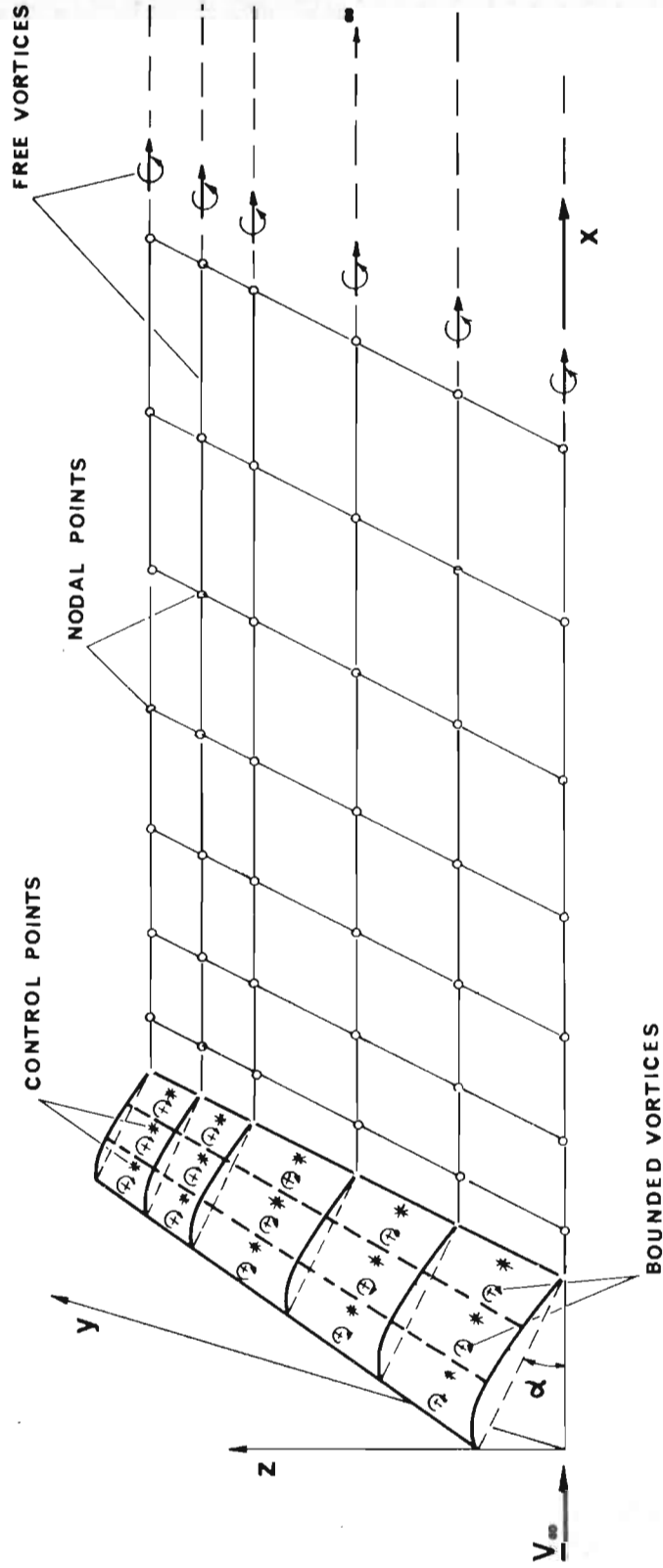


**Fig.1** Wing camber surface and wake representation by vortex distribution

**STEPS II&III**

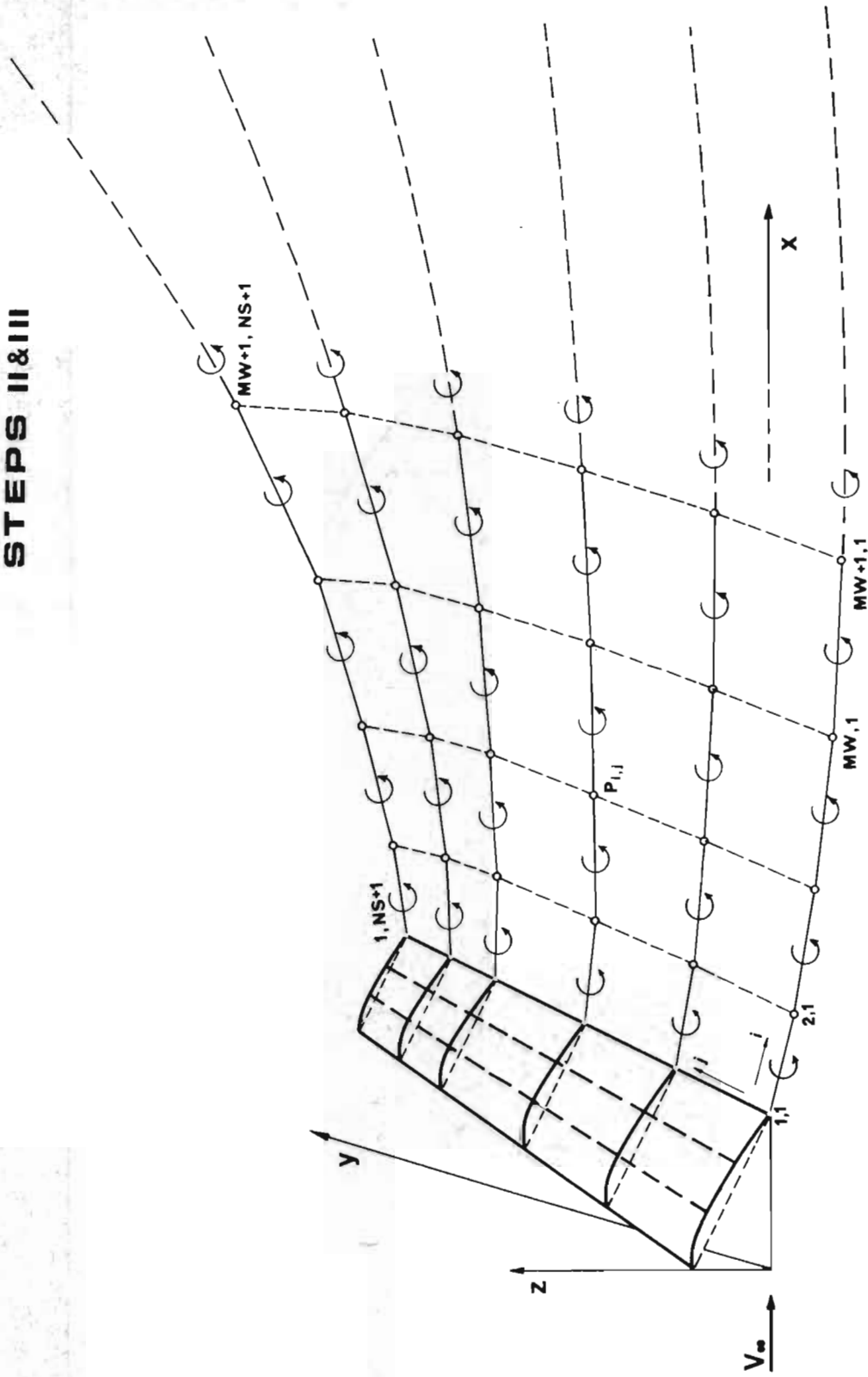


**Fig. 2** Trailing edge streamlines and free vortices position



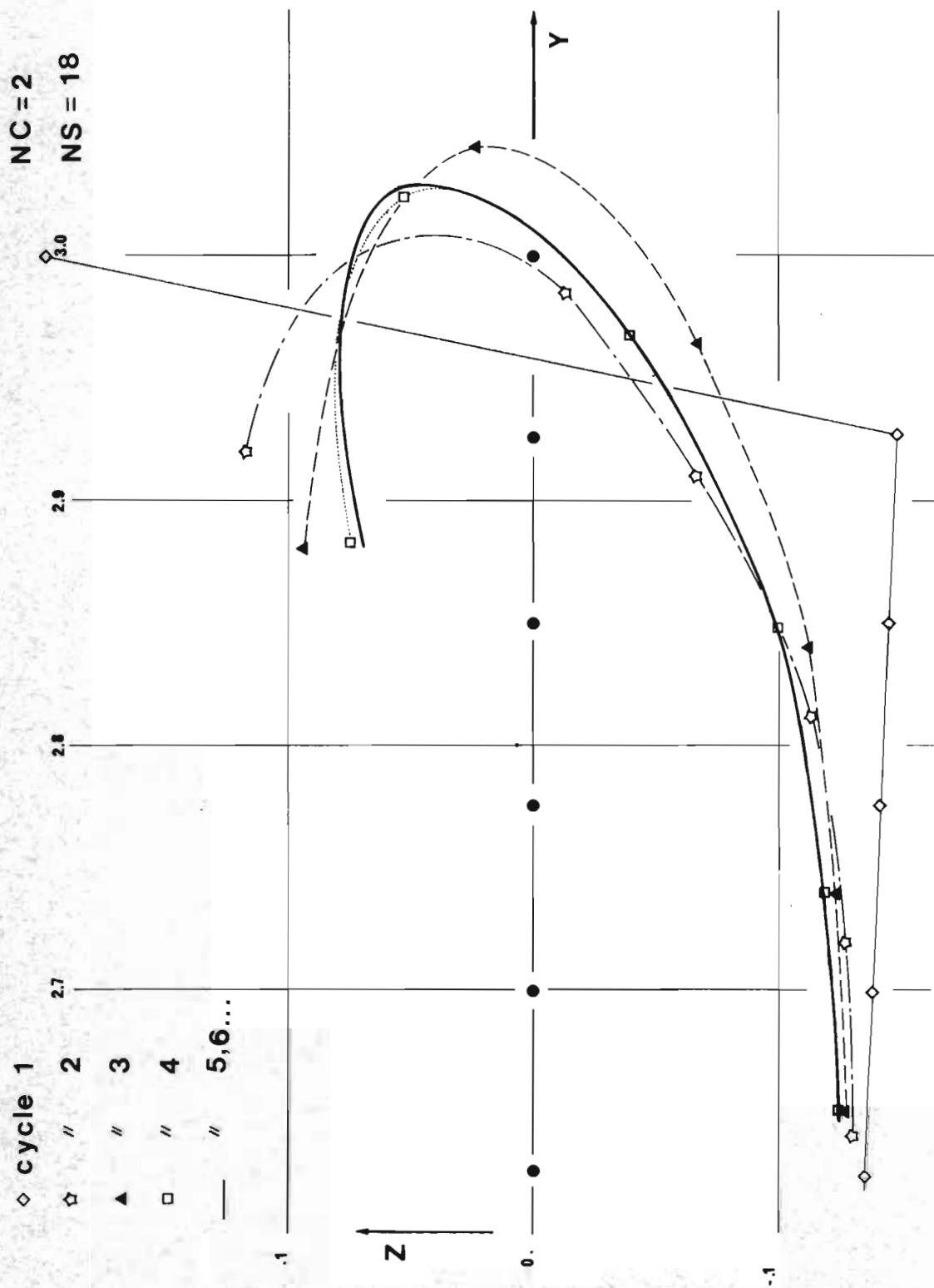


**Fig. 3** Rolling-up "story" for a wing with  $R = 6$ ,  $\alpha = 5^\circ$ , at  $x/c_R = 3$ , by FLT technique

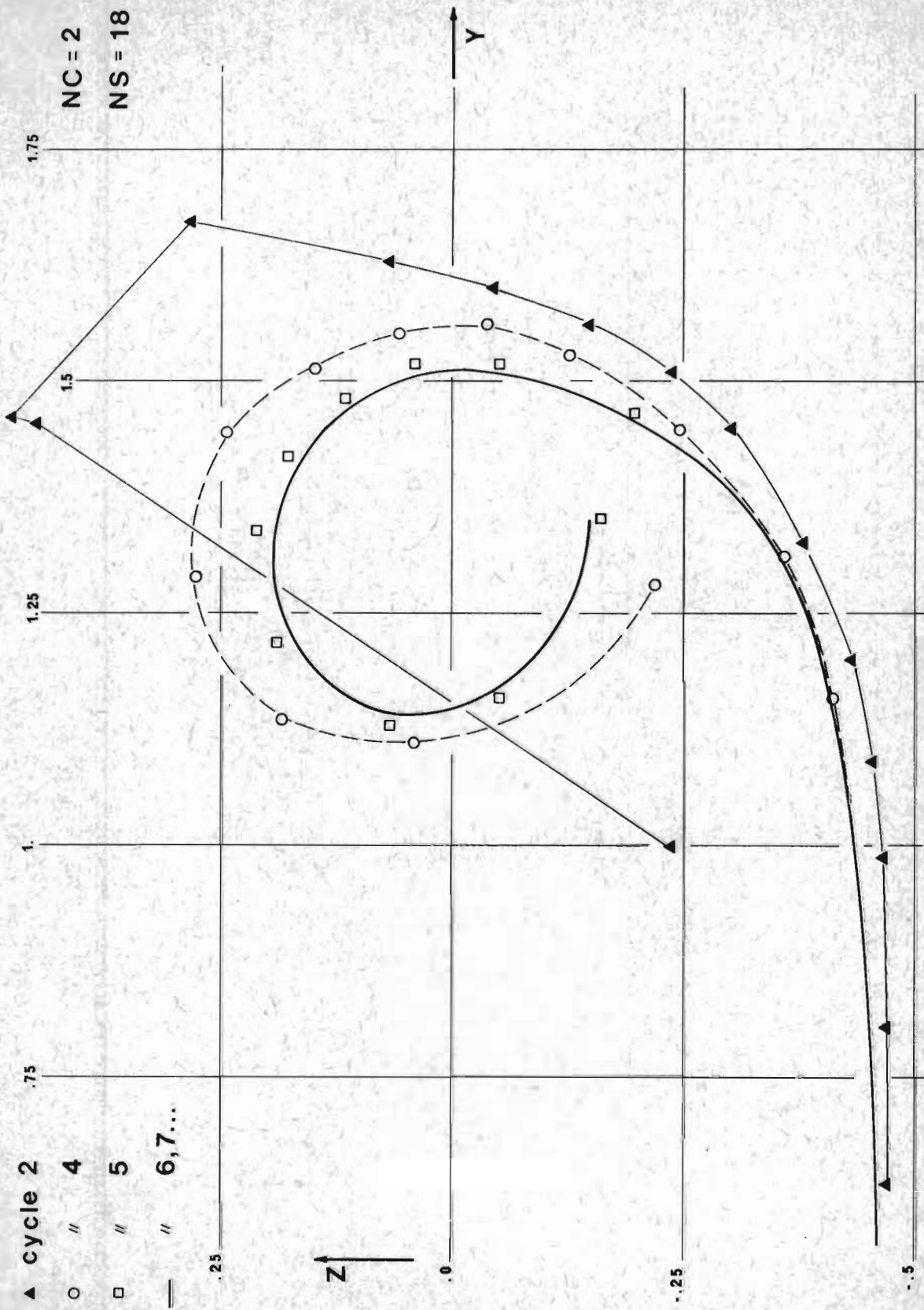


**Fig. 4** Rolling-up "story" for a wing with  $R = 3$ ,  $\alpha = 10^\circ$ , at  $x/c_R = 5$ .

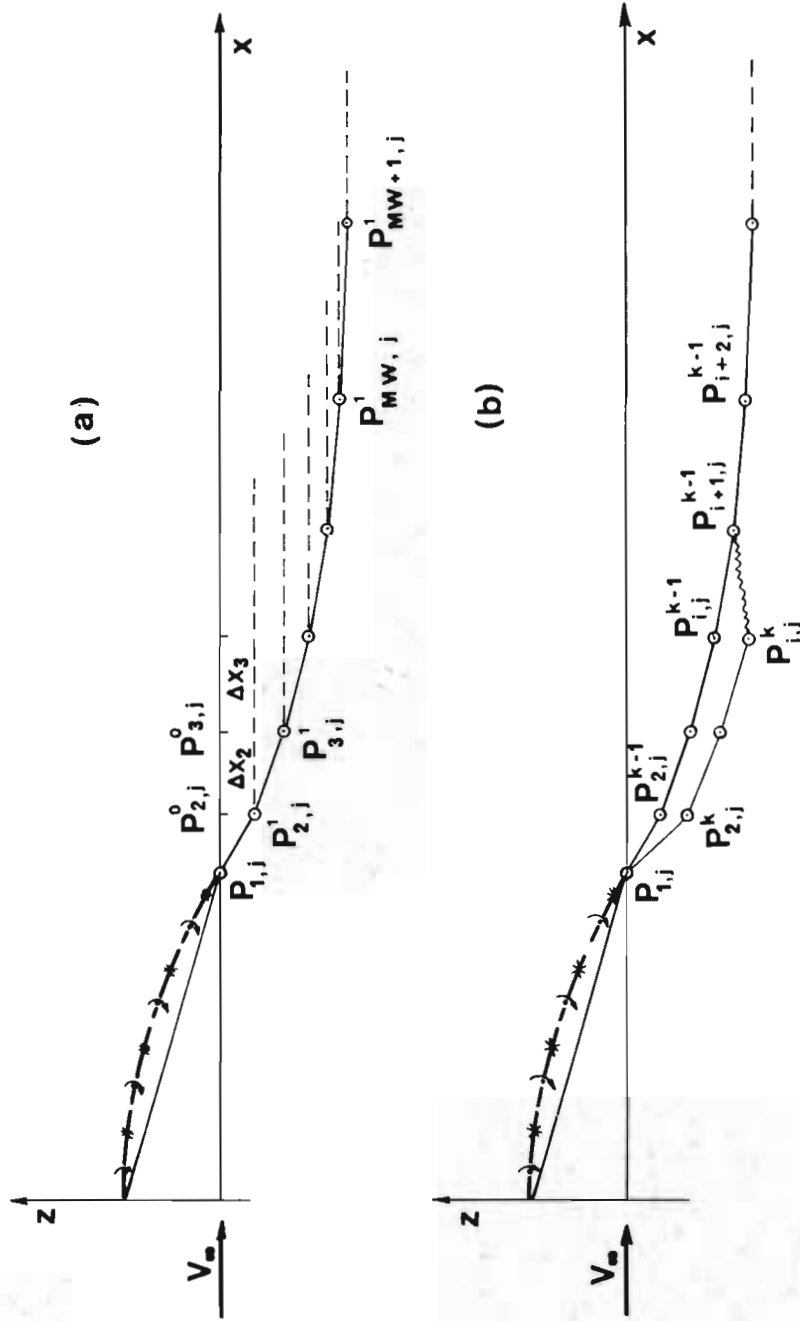


**Fig.5** RRT integration technique:  
 (a) streamline  $j$ -th at the first cycle  
 (b) " " " "  $k$ -th " "

NC = 2  
NS = 18

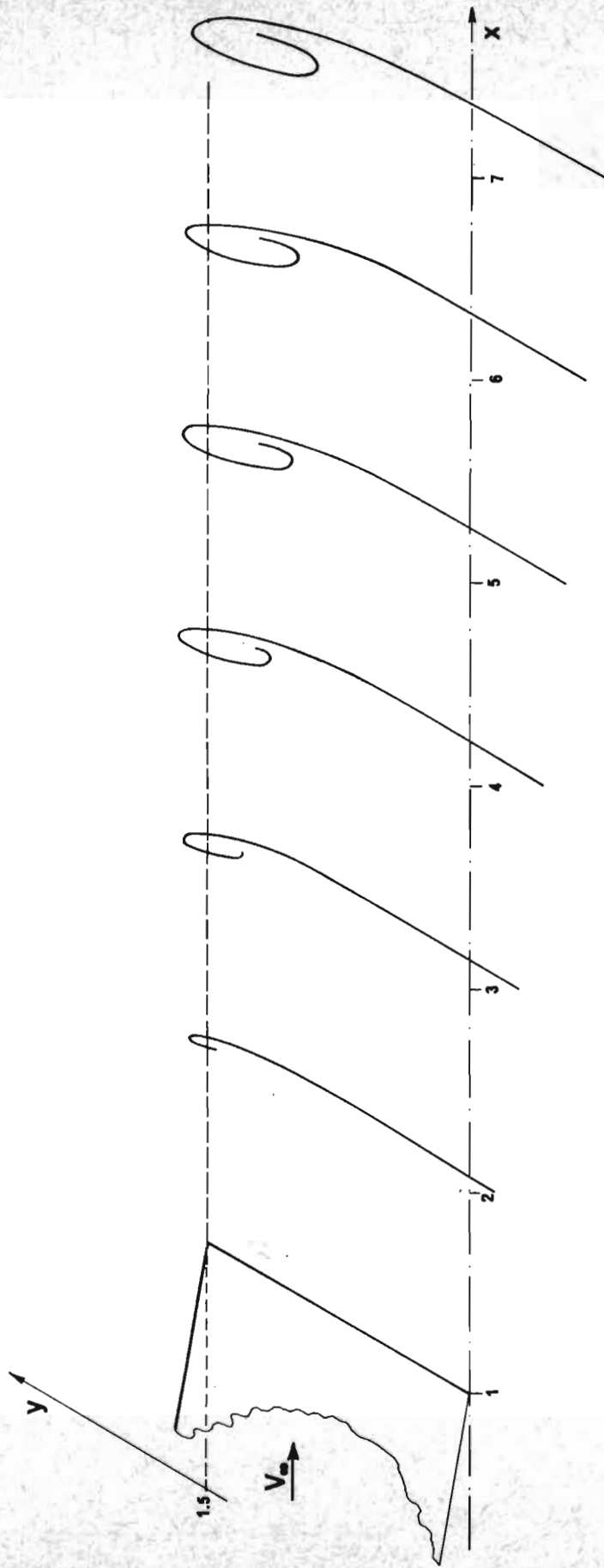


**Fig. 6** Wake view of a wing with  $R=3$  and  $\alpha = 10^\circ$ .

NC = 2  
NS = 18

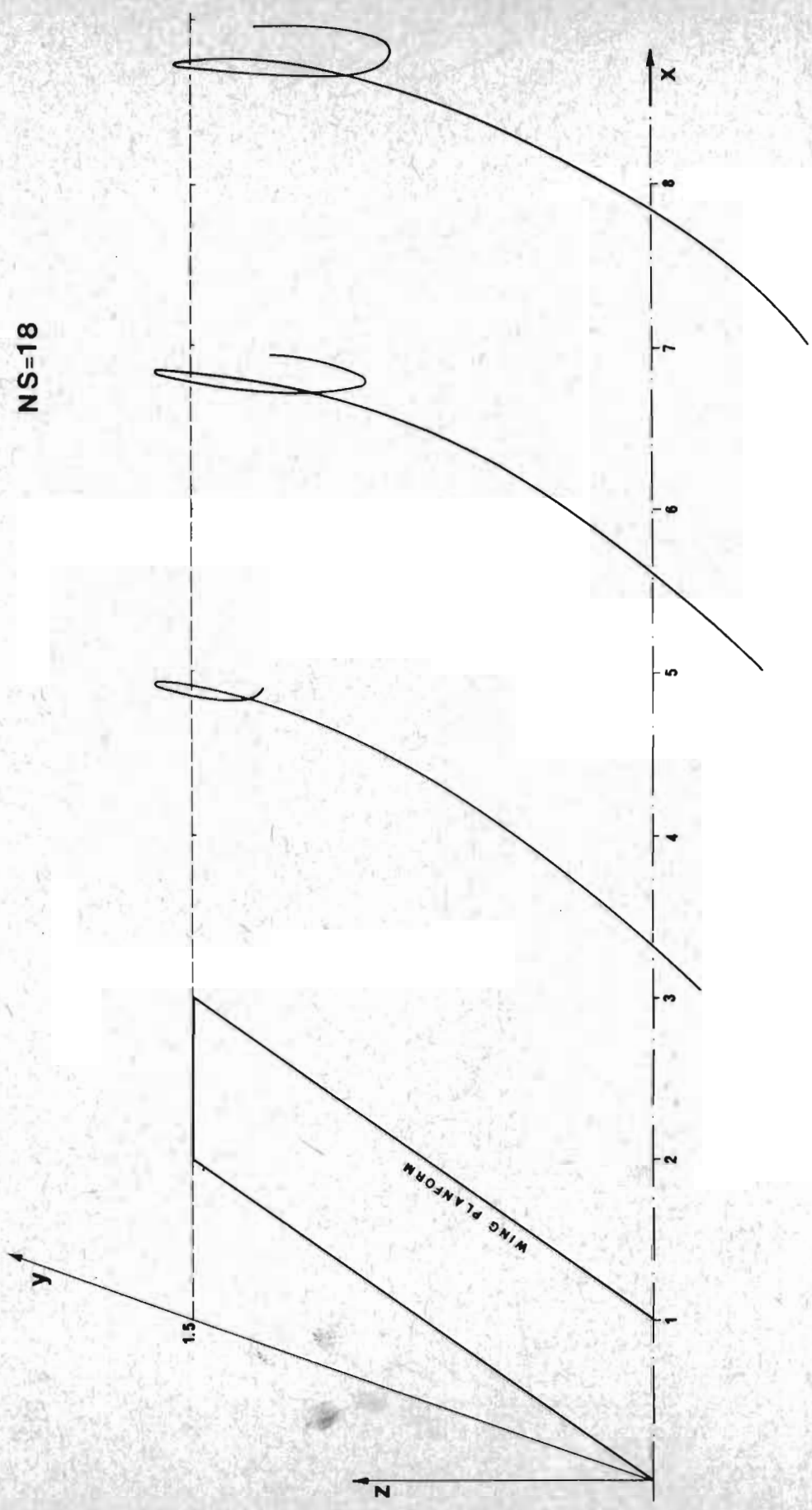
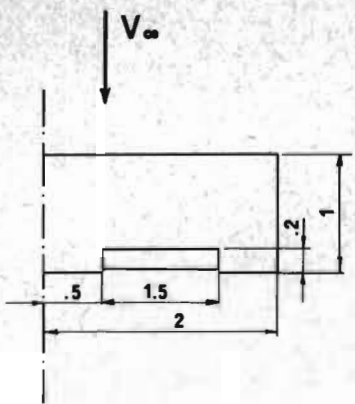
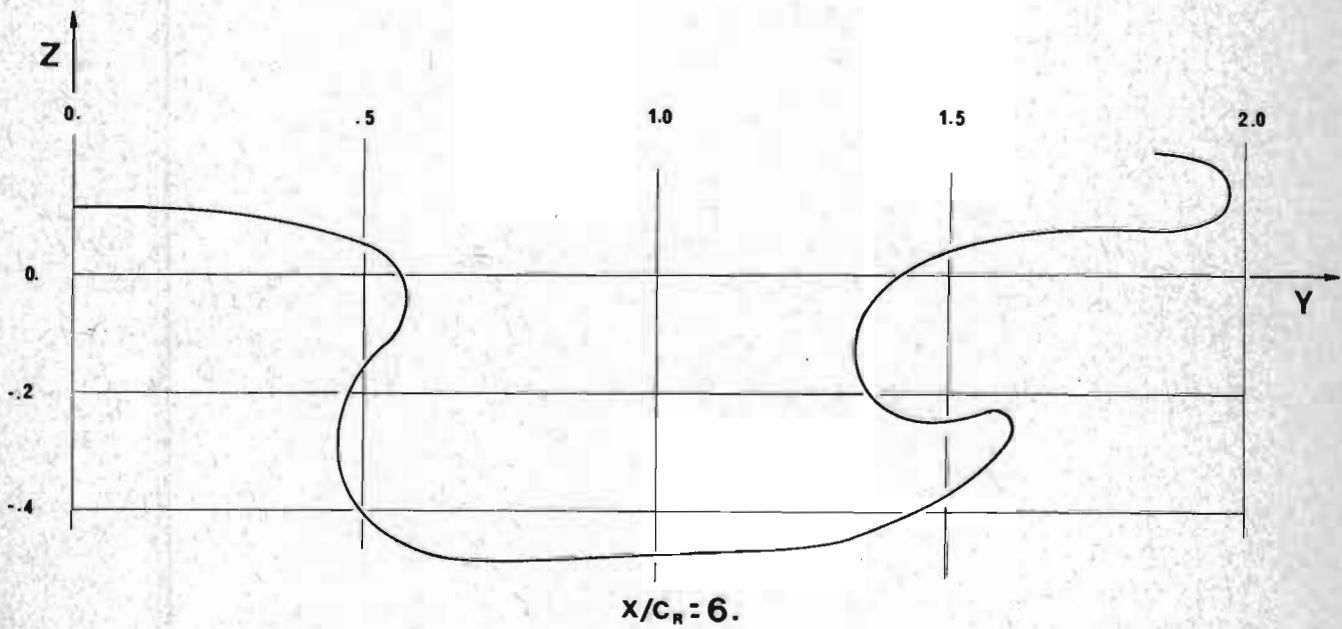
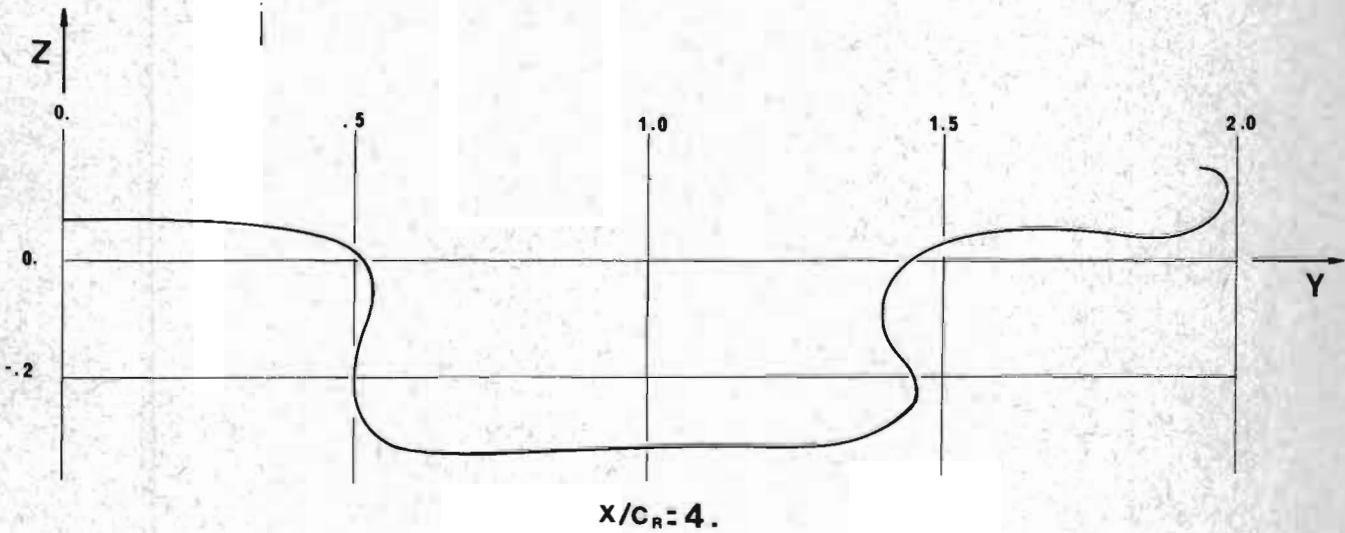


Fig. 7 Wake view of a wing with  $R = 3$ ,  $\alpha = 10^\circ$  and  $\Lambda_{LE} = 18.45^\circ$ .



$AR = 4$   
 $\alpha = 0^\circ$   
 $\delta_f = 10^\circ$   
 $NC = 4$   
 $NS = 29$



**Fig. 8** Rolling-up examples for a flapped rectangular wing.

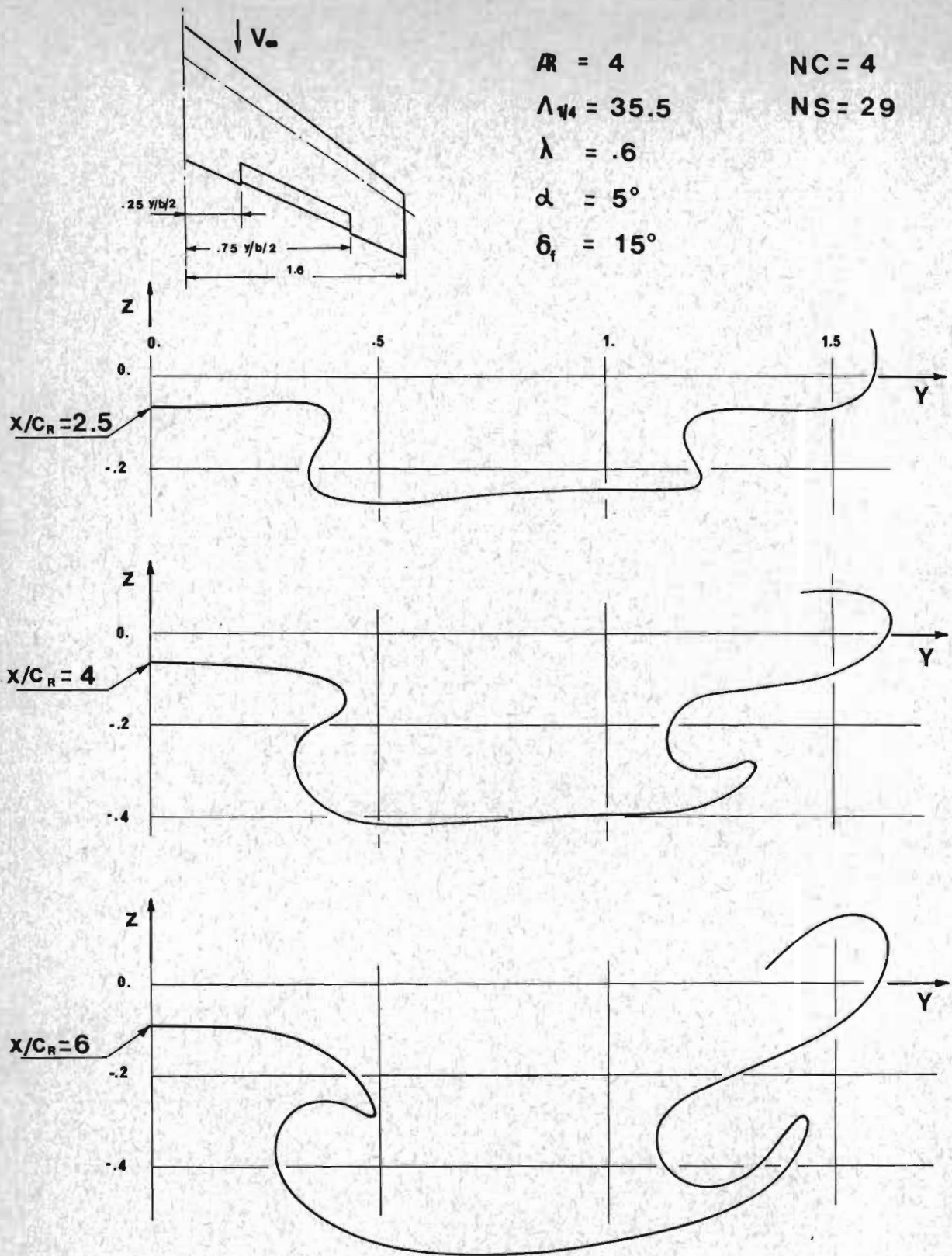


**Fig. 9** Roll-up rear view for a tapered swept flapped wing.

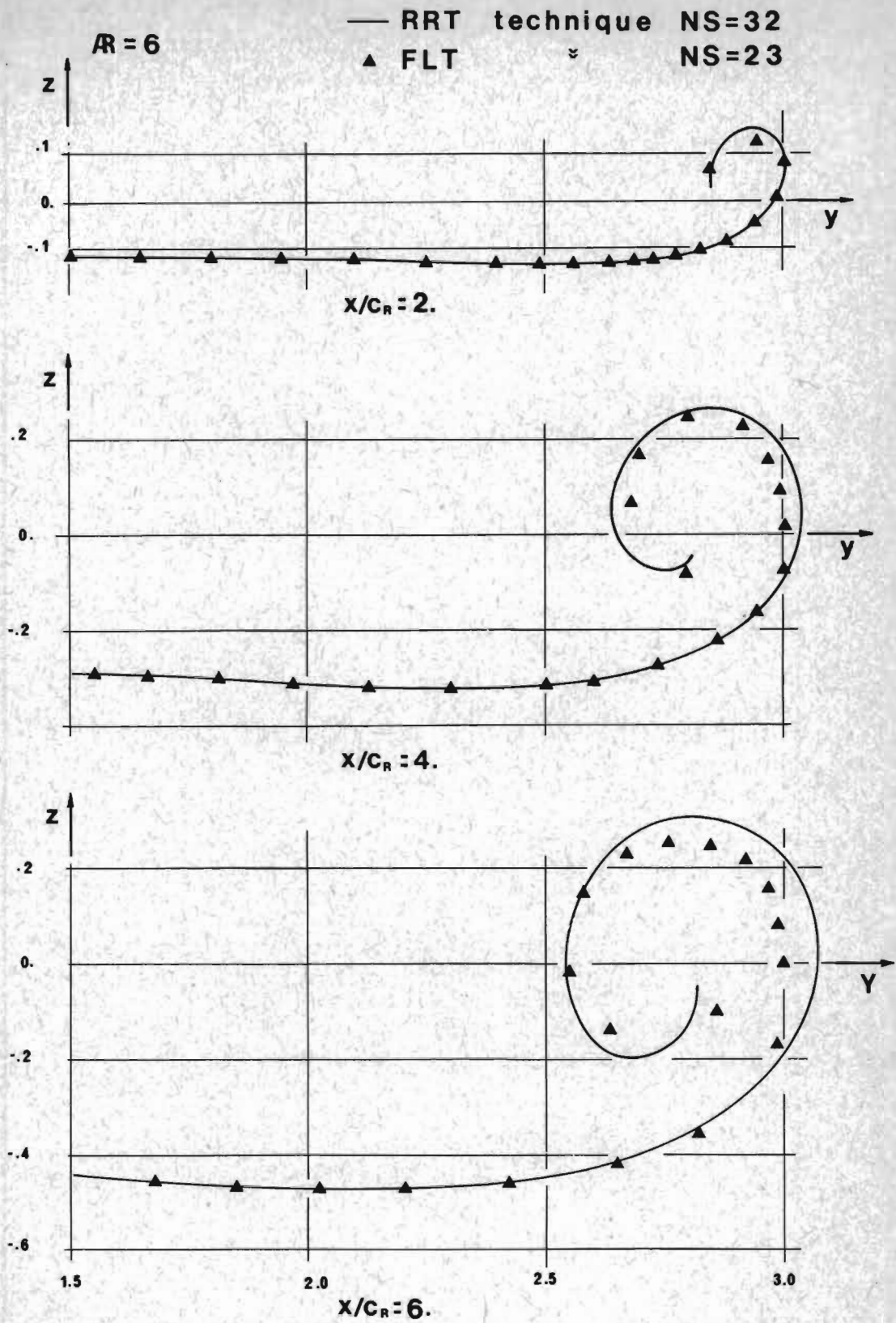


**Fig. 10** Comparisons of results between FLT and RRT techniques.



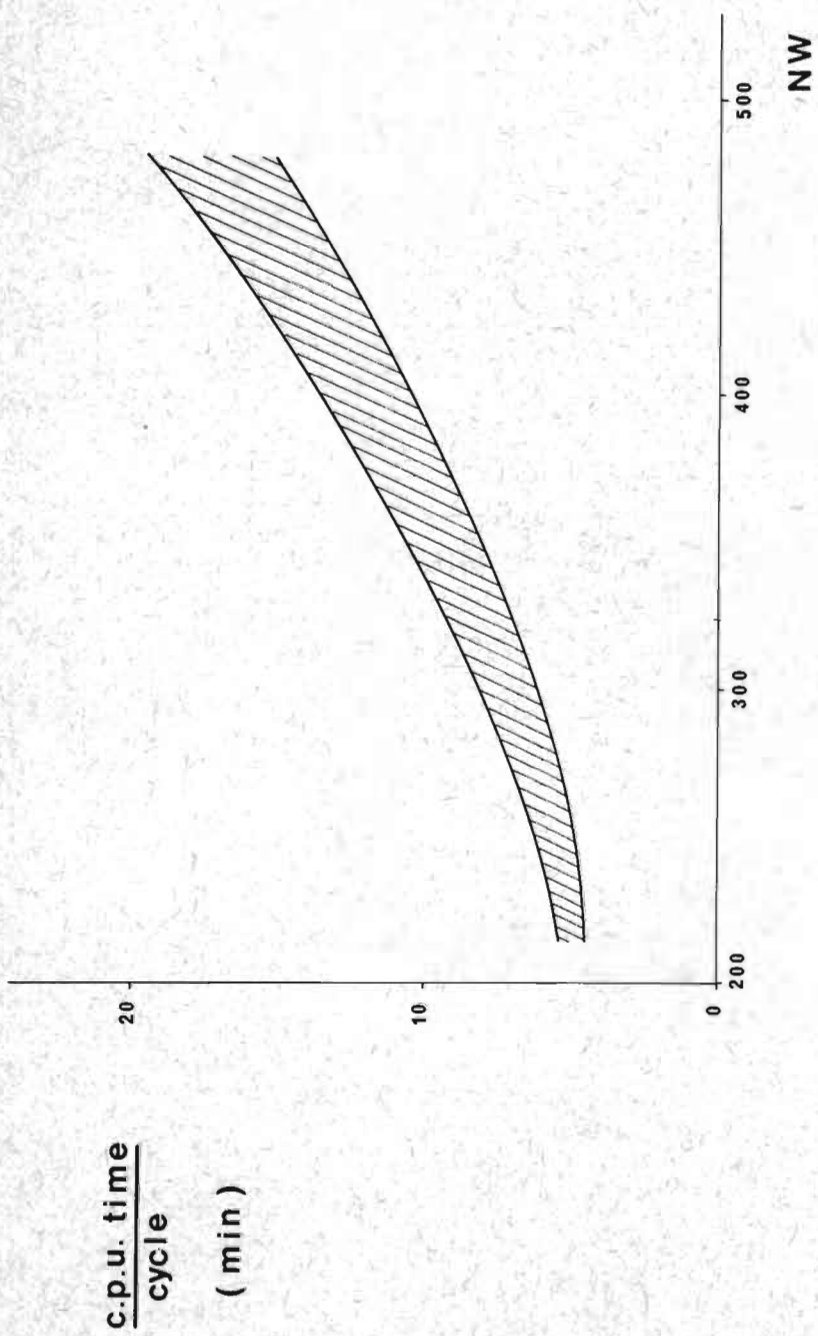


**Fig. 11** CPU time per cycle versus number of wake panels NW for the UNIVAC 1106 system

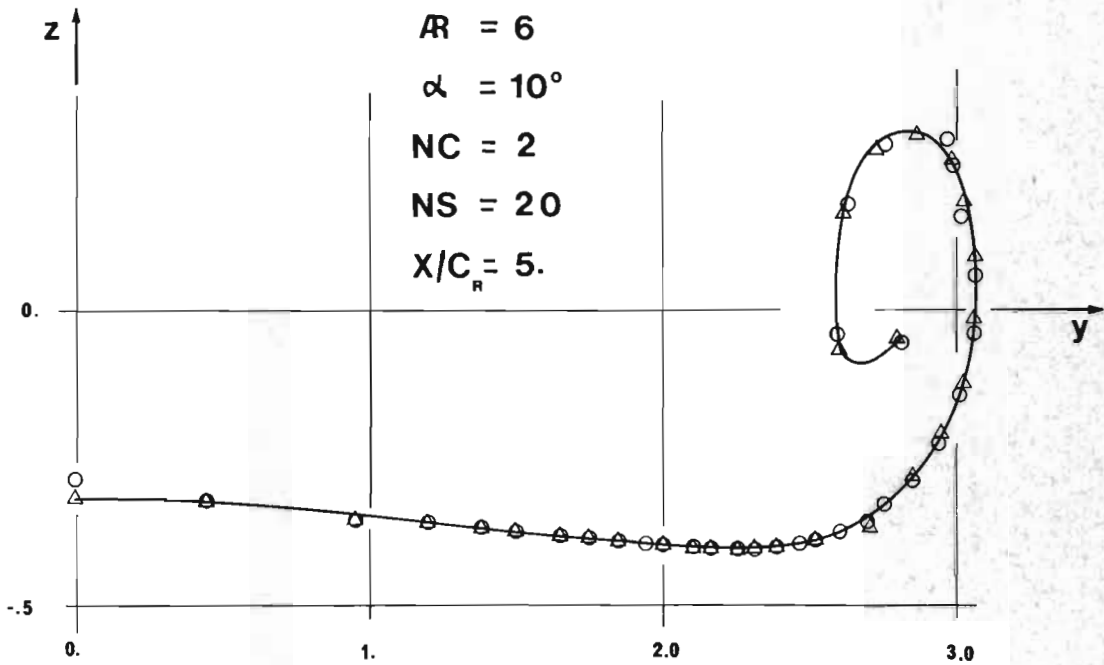
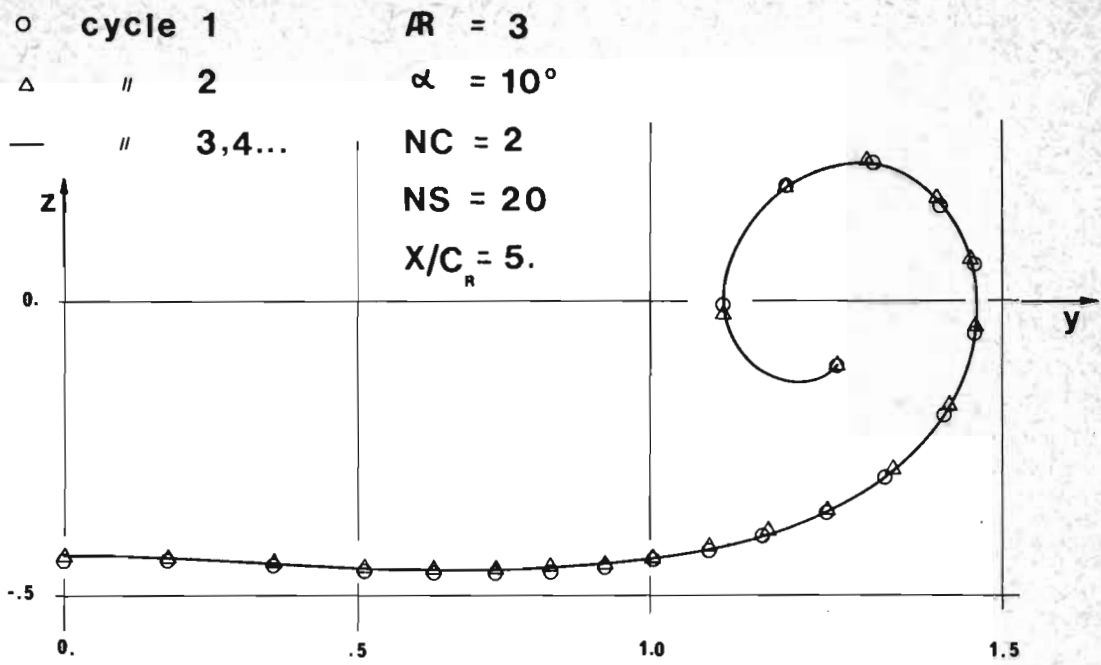


**Fig.12** RRT technique: rolling-up"story".

- cycle 2
- " 4
- ◆ " 5
- " 6,7...

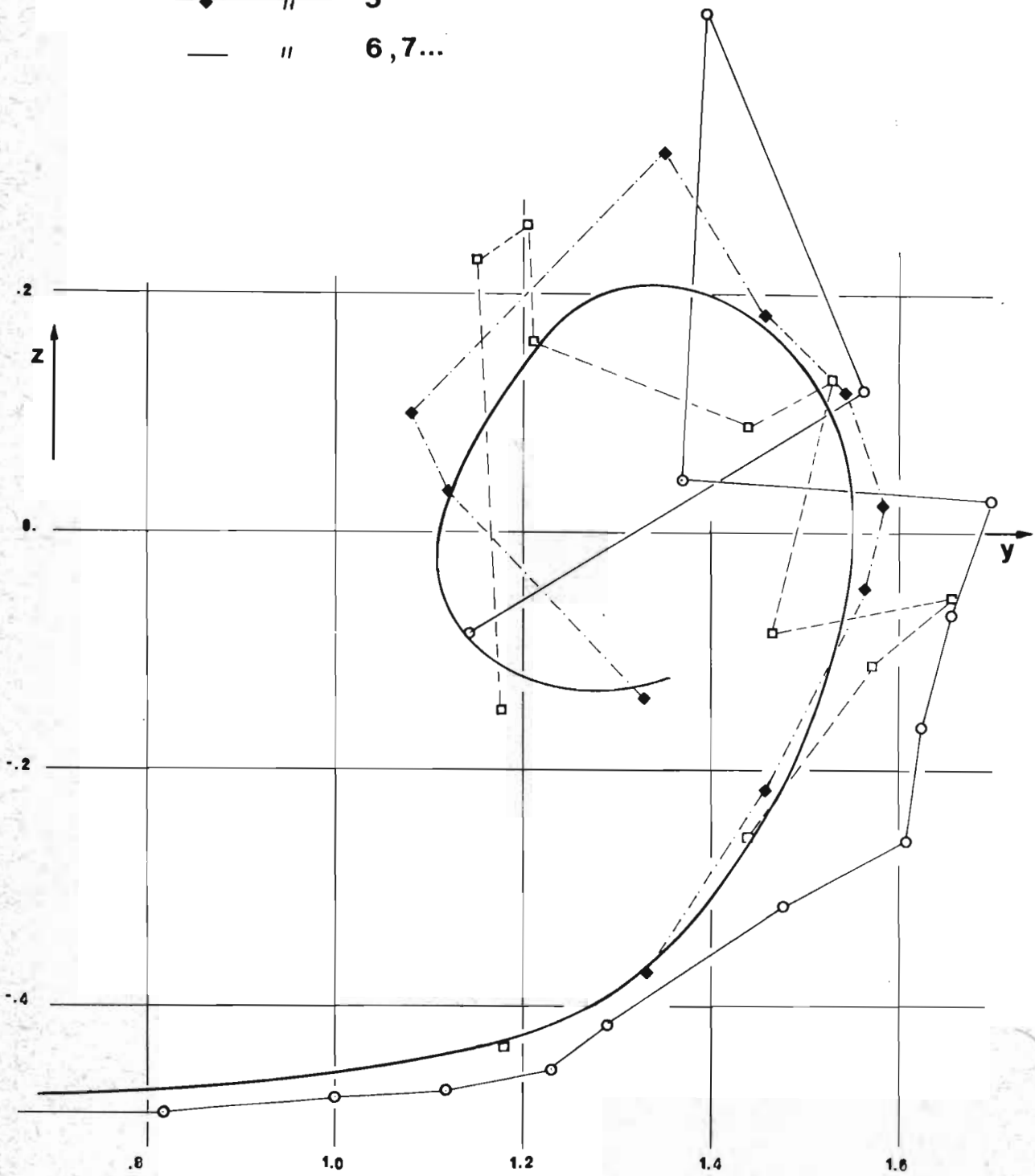


**Fig.13** Rolling-up "story" for an unplane wing with  $R = 3$ ,  $\alpha = 10^\circ$ , at  $x/c_R = 5$  by FLT technique.

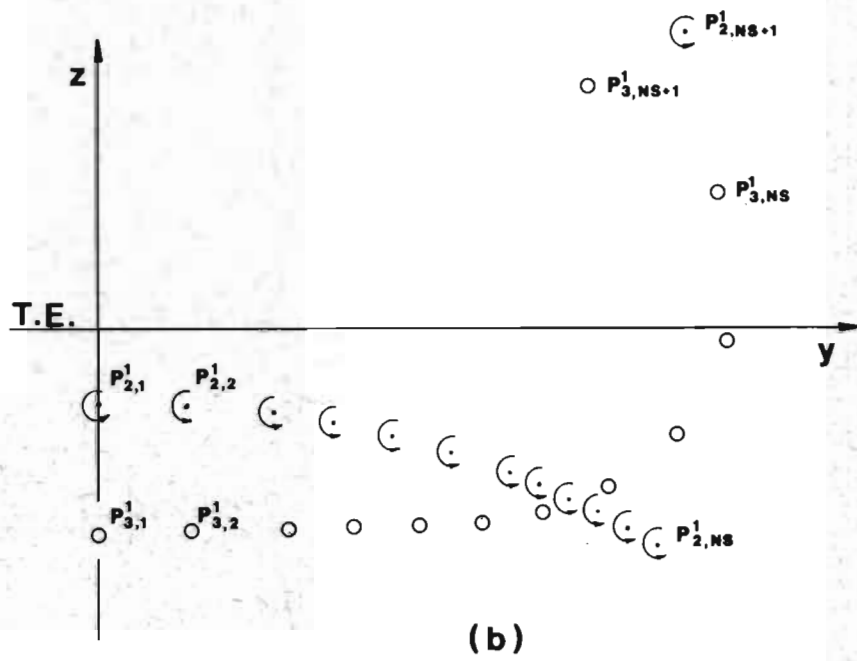
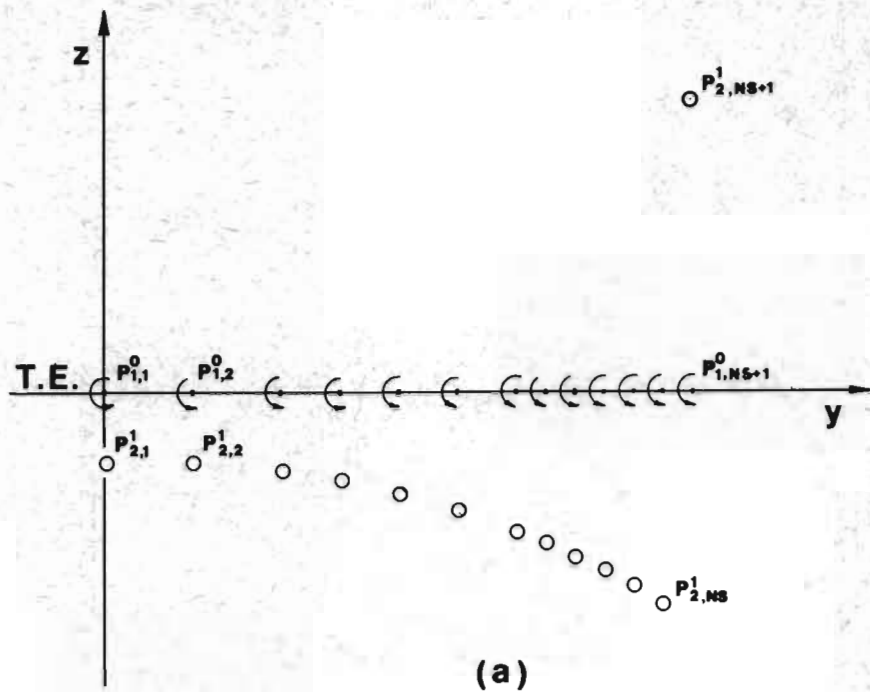


**Fig.14** Influence of mutual position among free vortices.

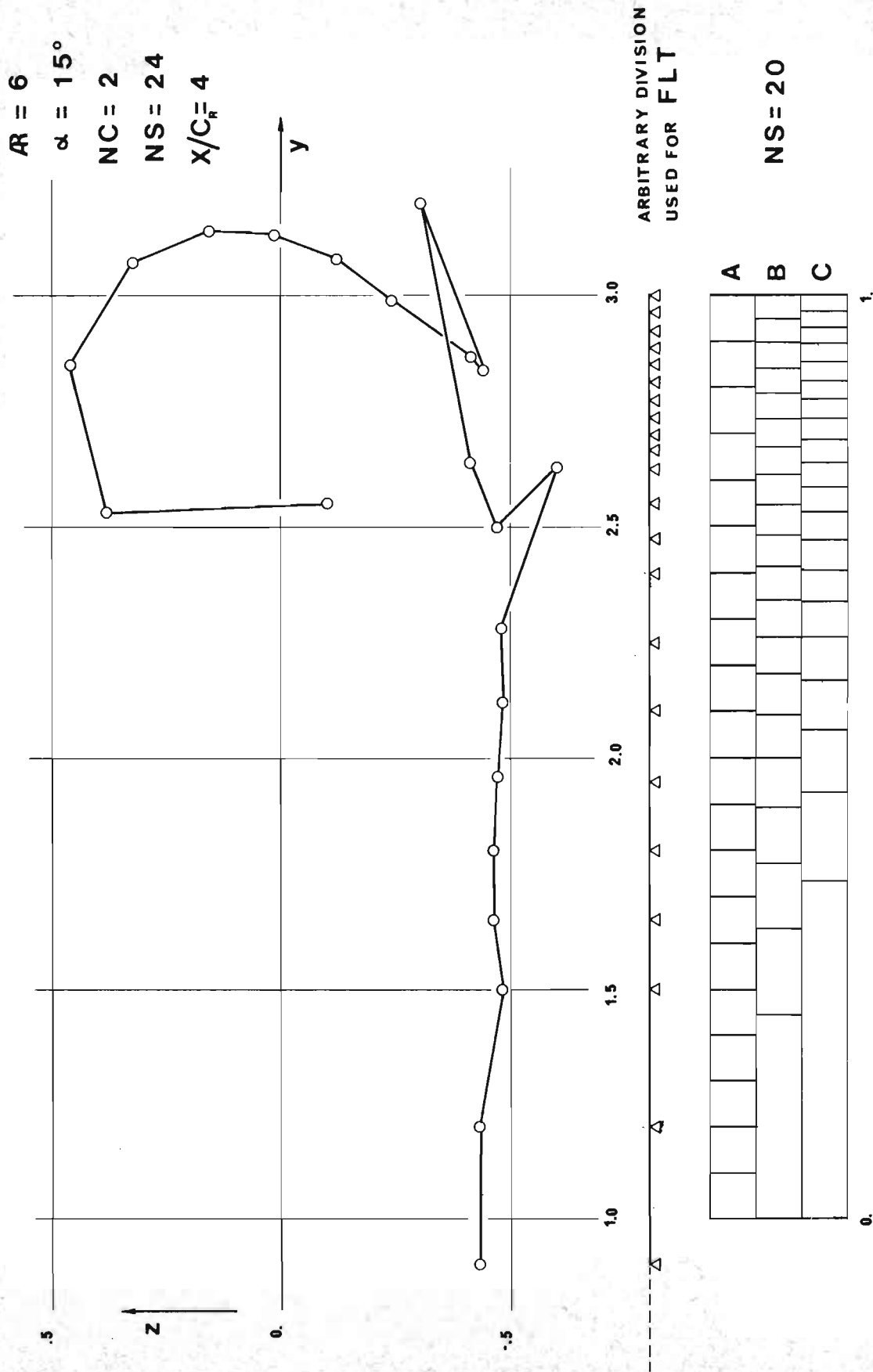


**Fig. 15** Cross-over of vortex lines and panel distribution types.

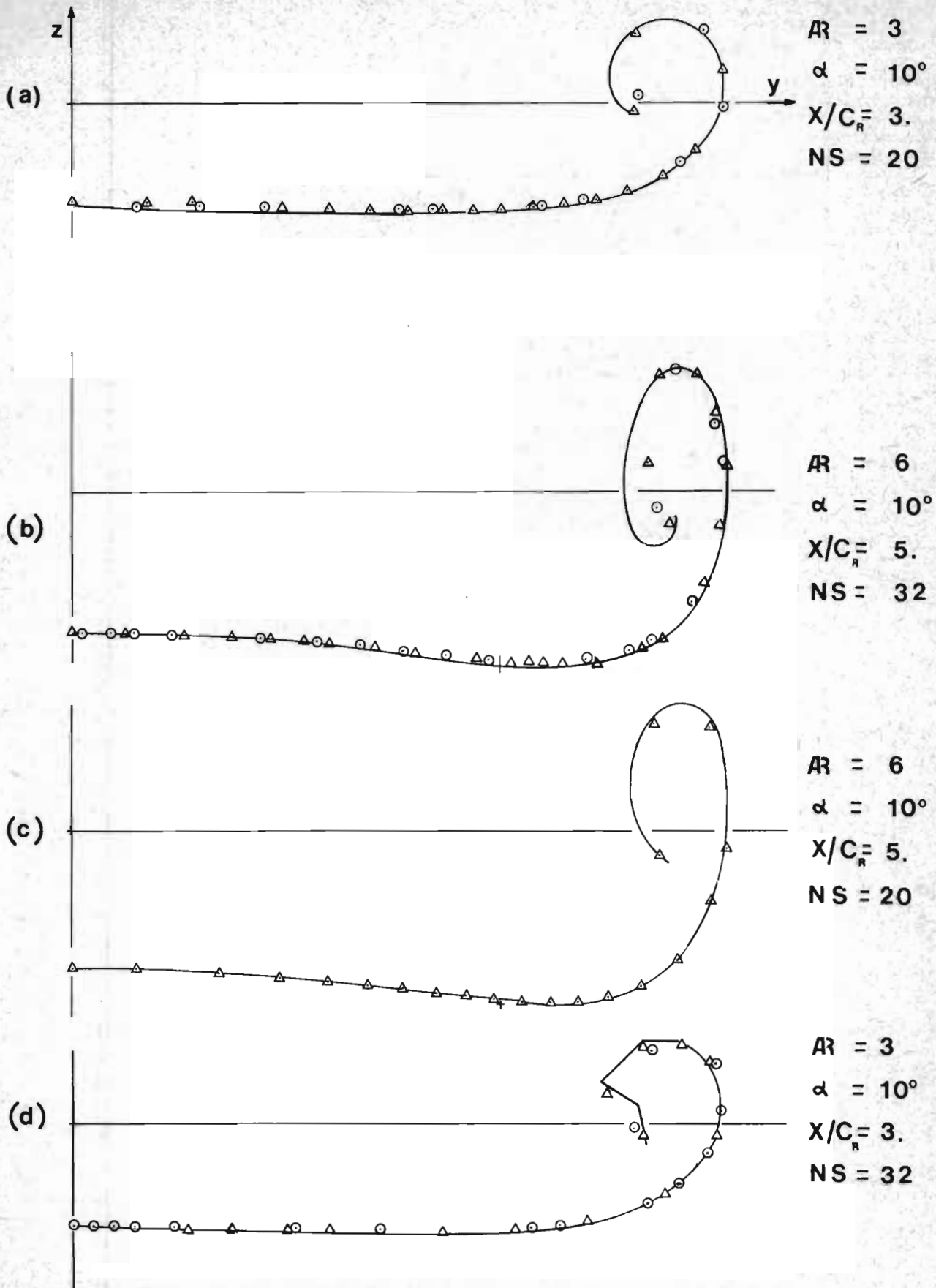


**Fig. 16** RRT technique: rolls-up obtained by panel distribution types A (O), B( $\Delta$ ) and C (continue line).

## D I S C U S S I O N

V.L. Marshall (British Aircraft Corporation, Weybridge, U.K. ): Some of the wake Locci calculations presented showed marked sharp curvatures in the cross-plane. This was noticeable with increased distance downstream and in addition was particularly strong when partial span flaps were introduced to the wing. The viscosity is expected to rationalize the pictures predicted by the computational model, so how accurate can we expect the results shown to be; for example in showing wake vortex core separation?

A. Mattei and E. Santoro: I agree completely on the fact that viscosity is expected to rationalize the pictures predicted by the method, especially for flapped wing, at large downstream distances. However, the aim of the work is not to compute the real wake versus time but to prepare an effective 3-D method that :

- (a) Resolves the potential wake problem in the manner that one can obtain stable and smooth rolling-up solutions.
- (b) Is useful for downwash computation on the tail in high lift configuration for which a 2-D approach fails and the viscosity influence is not noticeable.
- (c) Is able to be extended (e.g. Jet-flapped wing, low  $Re$  wings...).